Journal of the Serbian Society for Computational Mechanics / Vol. 7 / No. 1, 2013 / pp. 28-35

(UDC: 616-001.5-073:537.874.4)

Estimation of wave dispersion and attenuation for the assessment of healing bones

V. Potsika[1], V. Protopappas[2], M. Vavva[2], K. Raum[3], D. Rohrbach[3], D. Polyzos[2], D.I. Fotiadis[1]

[1] Unit of Medical Technology and Intelligent Information Systems, University of Ioannina, GR 45110 Ioannina, Greece
vpotsika@cc.uoi.gr, fotiadis@cc.uoi.gr
[2] Department of Mechanical Engineering and Aeronautics, University of Patras, GR 26500 Patras, Greece
vprotop@mech.upatras.gr, marvavva@gmail.com, polyzos@mech.upatras.gr
[3] Julius Wolff Institute, Berlin-Brandenburg School for Regenerative Therapies, Charité-Universitätsmedizin Berlin, Augustenburger Platz 1, 13353 Berlin, Germany
Kay.Raum@charite.de, Daniel.Rohrbach@charite.de

Abstract

Quantitative ultrasound has recently gained significant interest as a diagnostic tool of the bone healing process. Several multiple scattering theories have been proposed for the investigation of wave scattering in nonhomogeneous media, which however cannot provide realistic dispersion and attenuation estimations for different particle types and volume concentrations. In this study, we use an iterative effective medium approximation (IEMA) (Aggelis et al. 2004) to carry out wave dispersion and attenuation predictions in the callus region at different healing stages. The geometry and the material properties are derived from scanning acoustic microscopy images (SAM) of sheep healing tibia obtained at the third, sixth and ninth postoperative week (Anderson et al. 2008). The callus is assumed to be a composite medium consisted of blood and osseous tissue. The average particle diameters and the volume concentration were 350μm and 44.75% in week 3, 200μm and 38.67% in week 6, 120μm and 22.67% in week 9, respectively. Wave dispersion and attenuation are estimated for frequencies from 24 – 1200 kHz. Group velocity was found to decrease with increasing frequency, while the attenuation coefficient was found to increase in the examined frequency range. The results indicate that the scattering effects are more pronounced in the early healing stages. In conclusion, IEMA can provide reasonable predictions and could be thus exploited for bone healing assessment.

1. Introduction

The monitoring of the bone healing process using quantitative ultrasound is a promising non-destructive and non-radiating technique in terms of clinical diagnosis. Several research groups worldwide (Christensen 1990; Haïat et al. 2008) have studied the propagation of ultrasound in healing bones by performing measurements of the velocity and attenuation of the first arriving signal (FAS). However, the FAS corresponds to a lateral wave for wavelengths comparable to or smaller than the cortical thickness, thus reflecting only the periosteal region of bone. To this end, guided wave analysis was recently proposed as an effective method of bone assessment which is able to detect changes in bone and callus properties occurring at deeper layers (Christensen 1990

; Dodd et al. 2006). Nevertheless, further research is needed as the porous nature of callus which gives rise to multiple scattering phenomena during the healing process has neither been theoretically described nor numerically modeled for the purposes of ultrasound assessment.

Several numerical methods (Kim et al. 1995; Preininger et al. 2010) have been proposed for the quantitative determination of wave dispersion and attenuation in nonhomogeneous media based on the self-consistent theories. In these studies, the microstructure of the composite medium is assumed to be immersed into an infinitely extended effective medium. The frequency dependent wave velocity and attenuation coefficient are calculated by using self-consistent expressions most of which use scattering parameters derived from the solution of the single scattering problem. However, many of these theories are not able to provide reasonable wave dispersion and attenuation predictions for all types of suspensions and a wide range of particle concentrations and wavenumbers.

To this end, an iterative effective medium approximation (IEMA) was presented in (Aggelis et al. 2004; Laugier et al. 2011), aiming at the accurate evaluation of wave dispersion and attenuation in particulate composites, particle suspensions and emulsions, as well. The effectiveness of the methodology to provide reasonable predictions in composite materials including particles with volume concentrations up to 50% was demonstrated by comparing the numerical results of IEMA with experimental findings.

In this work, IEMA is used to perform wave dispersion and attenuation estimations in the callus region of healing bones at successive healing stages. Callus was assumed to be a porous, composite medium consisting of blood and osseous tissue. The material properties and the geometry of the callus were derived using serial scanning acoustic microscopy (SAM) images representing the third, sixth, ninth postoperative week (Anderson et al. 2008). Numerical calculations of the phase velocity and the attenuation coefficient are conducted in the frequency range from 24 – 1200 kHz. The numerical results show that the scattering effects are more pronounced in the early healing stages indicating that IEMA could provide supplementary information for the assessment of the healing process.

2. Materials and Methods

2.1. Scanning acoustic microscopy images

The SAM images illustrated in Fig. 1 were obtained from the right tibia of female Merino sheep and depict embedded longitudinal sections of a 3-mm osteotomy (Anderson et al. 2008). SAM is a non-invasive and non-destructive technique which uses ultrasound waves to detect changes in acoustic impedances occurring at the microstructural level and has been extensively used to investigate the elastic alterations of mineralized callus and cortical tissues (Anderson et al. 2008; Protopappas et al. 2007). Each SAM image represents a healing stage after three, six and nine weeks of consolidation. SAM measurements were derived using a spherically focused 50 MHz transducer with spatial resolution of 23 μm and scan increment of 16 μm.

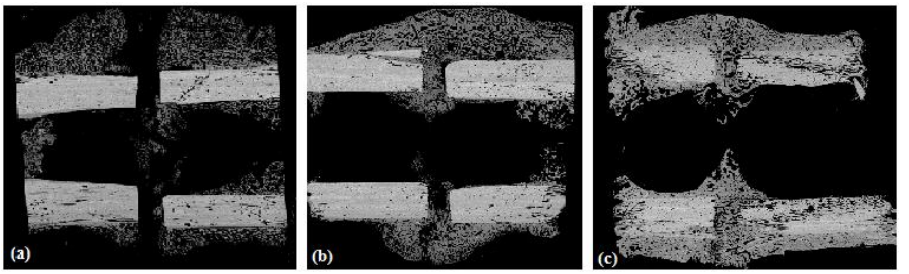

Fig. 1. SAM images representing: a) 3 weeks, b) 6 weeks and c) 9 weeks after the osteotomy.

2.2. The IEMA for particle suspensions

The propagation of a plane wave in nonhomogeneous media can be considered as a sum of a mean wave travelling in the medium with the dynamic effective properties of the composite and fluctuating waves induced by the multiple scattering of the mean wave. Under this consideration a complicated self-consistent multiple scattering condition can be applied to estimate the dynamic effective properties. In order to simplify the calculations, a simple self-consistent condition for composite media was proposed in (Kim et al. 1995):

$$n_1 g_d^{(1)}(\hat{\boldsymbol{d}};\hat{\boldsymbol{k}},\hat{\boldsymbol{k}}) + n_2 g_d^{(2)}(\hat{\boldsymbol{d}};\hat{\boldsymbol{k}},\hat{\boldsymbol{k}}) = 0, \tag{1}$$

where n_1, n_2 are the volume concentrations of the scatterers and the matrix, respectively, $\hat{\boldsymbol{k}}$ is the direction in which a $\hat{\boldsymbol{d}}$-polarized plane mean wave propagates and $g^{(1)}, g^{(2)}$ are the forward scattering amplitudes derived from the solution of the scattering problems 1 and 2, respectively, as illustrated in Fig. 2. The mean wave is both dispersive and attenuated. The complex wavenumber $k_d^{\,eff}(\omega)$ is defined as:

$$k_d^{\,eff}(\omega) = \frac{\omega}{C_d^{\,eff}(\omega)} + i\alpha_d^{\,eff}(\omega), \tag{2}$$

where $C_d^{\,eff}(\omega)$, $\alpha_d^{\,eff}(\omega)$ are the effective and frequency dependent phase velocity and attenuation coefficient, respectively, of a longitudinal (d ≡ P) or transverse (d ≡ S) mean wave propagating with circular frequency ω. In order to calculate $C_d^{\,eff}(\omega)$ and $\alpha_d^{\,eff}(\omega)$ the nonhomogeneous medium is replaced by an elastic homogeneous and isotropic material with bulk and shear moduli K^{eff} and μ^{eff}, respectively, calculated using the static mixture model of Christensen (Raum K et al. 2006):

$$K^{eff} = K_2 + \frac{n_1(K_1\text{-}K_2)(K_2+\frac{4}{3}\mu_2)}{n_2(K_1\text{-}K_2)+(K_2+\frac{4}{3}\mu_2)}, \tag{3}$$

$$A\left(\frac{\mu^{eff}}{\mu_2}\right)^2 + 2B\left(\frac{\mu^{eff}}{\mu_2}\right) + C = 0 \tag{4}$$

with A, B, C being functions of μ_1, μ_2, n_1 given in (Raum et al. 2006), while 1, 2 are indices corresponding to the material properties of the inclusion and the matrix, respectively. The effective density of the composite medium is defined as:

$$(\rho^{eff})_{step1} = n_1\rho_1 + n_2\rho_2. \tag{5}$$

The real effective wave number $(k_d^{eff})_{step1}$ of the mean wave can be estimated through the Eqs. (3), (4) and (5) and the relations:

$$C_p^{\,2} = (\lambda + 2\mu)/\rho, \tag{6}$$

$$C_s^{\,2} = \mu/\rho, \tag{7}$$

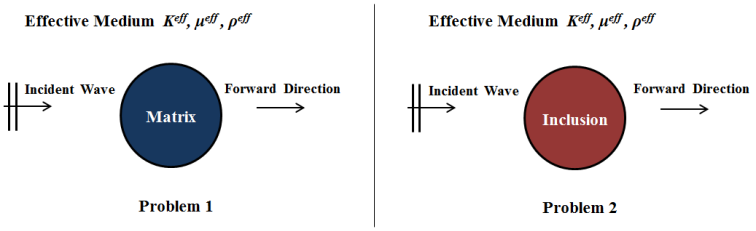

Fig. 2. A plane mean wave propagating in the effective medium and being scattered by: a) a matrix inclusion in problem 1, and b) a particle inclusion in problem 2.

where Cp and Cs are the longitudinal and the shear velocity of the propagated wave, respectively. Next, utilizing the material properties calculated in the first step, we proceed to the second step where the scattering problems 1 and 2, illustrated in Fig. 2, are solved in order to evaluate the forward scattering amplitudes $g^{(1)}, g^{(2)}$. Subsequently, the scattering amplitudes can be estimated according to the following equation:

$$g_d(\hat{\boldsymbol{d}};\hat{\boldsymbol{k}},\hat{\boldsymbol{k}}) = n_1 g_d^{(1)}(\hat{\boldsymbol{d}};\hat{\boldsymbol{k}},\hat{\boldsymbol{k}}) + n_2 g_d^{(2)}(\hat{\boldsymbol{d}};\hat{\boldsymbol{k}},\hat{\boldsymbol{k}}), \tag{8}$$

and making use of the dispersion relation proposed in (Machado et al. 2010), we can estimate the new effective wavenumber of the mean wave as:

$$(k_d^{eff})_{step2} = (k_d^{eff})_{step1} + \frac{3n_1 g_d(\hat{\boldsymbol{d}};\hat{\boldsymbol{k}},\hat{\boldsymbol{k}})}{\alpha^3 (k_d^{eff})_{step1}}, \tag{9}$$

where α is the radius of a volume equivalent to the particle sphere. The new complex density $(\rho^{eff})_{step2}$ is calculated based on the $(k_d^{eff})_{step2}$ and the Eqs. (3), (4), (6), (7). The second step is repeated with the material properties (3), (4) and the new density $(\rho^{eff})_{step2}$ until the self-consistent condition (Eq. (1)) to be satisfied. Thus, using the Eqs. (3), (9) the frequency dependent, effective phase velocity and attenuation coefficient of the mean wave can be calculated.

2.3. Material Properties

The material properties of each pixel composing the osseous tissues in Fig. 1 were derived using empirical equations. The density ρ was calculated using the equation (Tsinopoulos et al. 2000):

$$Z = 1.02\rho^{2.83} \tag{10}$$

where Z is the acoustic impedance.

Then, the elastic constant in the axial direction c_{33} is calculated via the equation (Tsinopoulos et al. 2000):

$$c_{33} = 2.75\rho^{3.99} \tag{11}$$

The Young modulus E is finally defined as (Anderson et al. 2008):

$$E = \frac{(1+\nu)(1-2\nu)}{(1-\nu)} c_{33} \tag{12}$$

	Osseous tissue (week 3)	Osseous tissue (week 6)	Osseous tissue (week 9)	Blood
ρ (kg/m^3)	1425	1729	1881	1055
E (GPa)	13.6	17.1	21.1	$3x10^{-3}$
λ (GPa)	7.9	9.9	12.2	2.6
μ (GPa)	5.2	6.6	8.1	$100x10^{-9}$

Table 1: Material properties of the callus components.

where ν is the Poisson's ratio. The callus tissue is considered isotropic with a Poisson's ratio ν = 0.3. The calculated average values of the callus material properties, as well as the material properties of blood are shown in Table 1 (Christensen 1990).

3. Results

Fig. 3 shows the group velocity and the attenuation coefficient predictions in the frequency range 24 – 1200 kHz for each healing stage. In Fig. 3a, the group velocity was found to decrease: a) from 1826 – 1609 m/s in week 3, b) from 2555 – 2403 m/s in week 6, and c) from 3202 – 3167 m/s in week 9. Fig. 3b shows an exponential increase of the attenuation coefficient with increasing frequency: a) from 0.06 – 76.36 m-1 in week 3, b) from 0 – 51.86 m-1 in week 6, and c) from 0 – 1.91 m-1 in week 9.

4. Discussion

In the present study, we used an iterative methodology to carry out wave dispersion and attenuation predictions in the callus region of healing long bones based on SAM images representing successive healing stages.

A negative dispersion is exhibited in all the examined healing stages. A similar phase velocity behavior has been previously observed by several research groups (Vavva et al. 2008; Waterman and Truell 1961) studying the porous structure of cancellous bone. Haït et al. (Vavva et al. 2008) suggested that this phenomenon is attributed to the coupling of multiple scattering and absorption effects due to the heterogeneity of the medium. Another possible explanation according to (Waterman and Truell 1961) is that negative dispersion can arise when signals consisted of overlapped fast and slow waves are analyzed as a single longitudinal wave.

In addition, we found that the group velocity and the attenuation coefficient derived from week 9 vary slightly with increasing frequency in comparison to weeks 3 and 6. This could be attributed to the consolidation of the callus tissue at the final healing stages, followed by

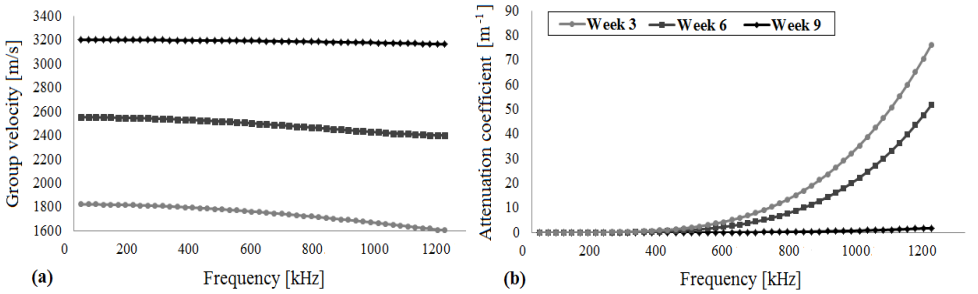

Fig. 3. Estimation of: a) the group velocity and b) attenuation coefficient for each healing stage.

a gradual decrease of the particles' volume concentration and diameter. Thus, the role of scattering and absorption effects is more pronounced during the early healing stages. Our findings indicate that IEMA provides reasonable results and could be used for the evaluation of bone healing.

However, the presented results concern exclusively the callus tissue, thus neglecting the cortical bone. In our future work the effective material properties and the attenuation coefficient calculated from IEMA will be incorporated to numerical models of healing long bones using the boundary element method in order to simulate wave propagation.

5. Conclusions

In this work, we presented group velocity and attenuation predictions in healing long bones based on an iterative effective medium approximation. For the first time, wave dispersion and attenuation were quantitatively determined in the composite geometry of the callus at different healing stages. This study constitutes a starting point for the systematic investigation of the scattering effects induced by the porous nature of callus at different healing stages. However, the results should be interpreted with caution as further theoretical and numerical research is needed.

Извод

Одређивање дисперзије и слабљења таласа за процену процеса зарастања костију

V. Potsika[1], V. Protopappas[2], M. Vavva[2], K. Raum[3], D. Rohrbach[3], D. Polyzos[2], D.I. Fotiadis[1]

[1]Unit of Medical Technology and Intelligent Information Systems,University of Ioannina, GR 45110 Ioannina, Greece
vpotsika@cc.uoi.gr, fotiadis@cc.uoi.gr
[2] Department of Mechanical Engineering and Aeronautics, University of Patras, GR 26500 Patras, Greece
vprotop@mech.upatras.gr, marvavva@gmail.com, polyzos@mech.upatras.gr
[3] Julius Wolff Institute, Berlin-Brandenburg School for Regenerative Therapies, Charité-Universitätsmedizin Berlin, Augustenburger Platz 1, 13353 Berlin, Germany
Kay.Raum@charite.de, Daniel.Rohrbach@charite.de

Резиме

Квантитативни ултразвук завређује све више пажње као дијагностичко средство у процесу зарастања костију. Неколико теорија вишеструког расејања предложене су за испитивање расипања таласа у нехомогеним медијима, које, међутим, не могу да пруже реалистичне процене дисперзије и слабљења за различите врсте честица и запреминске концентрације. У овом истраживању, користимо итеративну ефикасну апроксимацију медија (IEMA) (Aggelis et al. 2004) како бисмо извршили предвиђања расипања и слабљења у регији калуса у различитим фазама излечења. Геометрија и материјална својства изведене су из слика скенинг акустичне микроскопије (SAM) потколенице код оваца, у фази излечења, добијених у трећој, шестој и деветој седмици након операције (Anderson C C et al. 2008). Претпоставља се да је калус композитни медиј који се састоји од крви и коштаног ткива. Просечни пречници честица и запреминска концентрација били су 350μm и 44.75% у трећој седмици, 200μm и 38.67% у шестој седмици, 120μm и 22.67% у деветој седмици, респективно. Расипање и слабљење таласа се процењују за фреквенције од 24 – 1200 kHz. Увидели смо да се групна брзина смањује са повећањем фреквенције, док се коефицијент слабљења повећава у испитиваном опсегу фреквенције. Резултати указују на то да су ефекти расипања израженији у ранијим фазама лечења. Закључак је да IEMA може пружити оправдана предвиђања и стога може бити коришћена за процену излечења костију.

References

Aggelis D. G., Tsinopoulos, S. V., Polyzos D., (2004). An iterative effective medium approximation for wave dispersion and attenuation predictions in particulate composites, suspensions and emulsions, *J. Accoust. Soc. Am*., 9, pp. 3443–3452.

Anderson C. C., Marutyan K. R., Holland M. R., Wear K. A., Millera J. G., (2008). Interference between wave modes may contribute to the apparent negative dispersion observed in cancellous bone, *J. Acoust. Soc. Am.*, 124, 1781–1789.

Christensen R. M., (1990). A critical evaluation for a class of micromechanics models, *J. Mech. Phys. Solids*, 38, pp. 379-404.

Dodd S. P., Cunningham J. L., Miles A. W., Gheduzzi S., Humphrey V. H., (2006). An in vitro study of ultrasound signal loss across simple fractures in cortical bone mimics and bovine cortical bone samples, *Bone*, 40, pp. 656–661.

Foldy L. L., (1945). The multiple scattering of waves, *Phys. Rev.*, 67, pp. 107–119.

Haïat G., Lhemery A., Renaud F., Padilla F., Laugier P., Naili S., (2008). Velocity dispersion in trabecular bone: influence of multiple scattering and of absorption, *J. Acoust. Soc. Am.*, 124, pp. 4047‑4058.

Kim J. Y., Ih J. G., Lee B. H., (1995). Dispersion of elastic waves in random particulate composites, *J. Acoust. Soc. Am.*, 97, pp. 1380–1388.

Laugier P. and Haiat G., (2011). Bone quantitative ultrasound, Springer Dordrecht Heidelberg London New York: Science+Business Media B.V., pp. 409–440.

Machado C. B., Albuquerque Pereira W. C., Talmant M., Padilla F., Laugier P., (2010). Computational evaluation of the compositional factors in fracture healing affecting ultrasound axial transmission measurements, *Ultrasound in Med. & Biol.*, 36, pp. 1314–1326.

Preininger B., Checa S., Molnar F. L., Fratzl P., Duda G. N., Raum K., (2011). Spatial-temporal mapping of bone structural and elastic properties in a sheep model following osteotomy, *Ultrasound in Med. & Biol.*, 37, pp. 474–483.

Protopappas V. C., Kourtis I. C., Kourtis L. C., Malizos K. N., Massalas C. V., Fotiadis D. I., (2007). Three dimensional finite element modeling of guided ultrasound wave propagation in intact and healing long bones, *J. Accoust. Soc. Am.*, 121, pp. 3907–3921.

Raum K., Cleveland R. O., Peyrin F., Laugier P., (2006). Derivation of elastic stiffness from site-matched mineral density and acoustic impedance, *Phys. Med. Biol.*, 51, pp. 747–758.

Tsinopoulos S. V., Verbis J. T., Polyzos D., (2000). An iterative effective medium approximation for wave dispersion and attenuation predictions in particulate composites, *Adv. Composite Lett.*, 9, pp. 193-200.

Vavva M. G., Protopappas V. C., Gergidis L. N., Charalambopoulos A., Fotiadis D. I., Polyzos D., (2008). The effect of boundary conditions on guided wave propagation in two-dimensional models of healing bone, *Ultrasonics*, 48, pp. 598–606.

Waterman P. C. and Truell R., (1961). Multiple scattering of waves, *J. Math. Phys.*, 2, pp. 512-537.